

# END TO END BEAM DYNAMICS AND DESIGN OPTIMIZATION FOR CSNS LINAC

J. Peng, H.C. Liu, X.J. Yin, H.F. Ouyang, S.N. Fu, IHEP, Beijing 100049, China

## Abstract

The China Spallation Neutron Source (CSNS) will use a linear accelerator delivering a 15mA beam up to 80MeV for injection into a rapid cycling synchrotron (RCS). Since each section of the linac was determined individually, a global optimization based on end-to-end simulation results has refined some design choices, including the drift-tube linac (DTL) and the medium energy beam transport (MEBT). The simulation results and reasons for adjustments are presented in this paper.

## INTRODUCTION

The layout of CSNS linac is sketched in Figure 1. It consists of a 50 keV  $H^-$  Penning surface plasma ion source, a 3MeV Radio Frequency Quadrupole (RFQ) accelerator, an 80MeV Alvarez-type Drift Tube Linear Accelerator (DTL) and several beam transport lines. The beam current of the linac is about 15mA with a pulsed beam width about 420  $\mu$ s and a repetition rate of 25Hz.

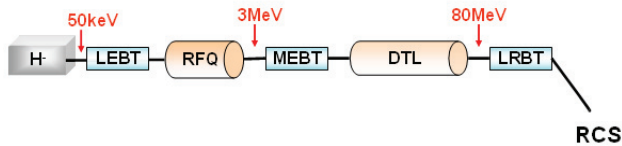


Figure 1: Layout of CSNS linac.

An electrostatic deflector as the pre-chopper, which is installed downstream LEFT, i.e., the entrance of RFQ, is chosen to pre-chop the beam in the rise and fall times of 15~20ns. Four-vane type RFQ is adopted to accelerate the  $H^-$  beam from 50keV to 3.0MeV. The length of RFQ is about 3.6m. The RFQ consists of two resonantly coupled sections, and each section includes two mechanical modules connecting together by flange [1]. The MEBT is a complex beam transport line. Its main role is to perform transverse and longitudinal matching to the succeeding 324MHz DTL. The MEBT includes ten quadrupole magnets (Q1~Q10) for transverse matching, two 324MHz buncher cavities for longitudinal matching, and various beam diagnostic instrumentations for beam diagnosis. The DTL consists of 4 tanks operating at 324MHz with final output energy of 80MeV. The transverse focusing is arranged in an FFDD lattice utilizing electro-magnet quadrupoles. The line to RCS beam transport line (LRBT) transfers the  $H^-$  beam from the linac injector to the RCS ring [2]. The layout here described is the result of several revisions of previous designs [3], the main changes being in the control of beam loss.

## BEAM LOSS STUDY

Each section of CSNS linac has been studied and optimized independently at the beginning of design. After

an initial layout of the accelerator is produced, a campaign of end to end simulation is launched with the purpose of identifying bottlenecks, weak points and acceptance limitations. The codes PARMILA [4] and PARMTEQM [5] have been used for these studies. From the results of simulation, we found that the 1<sup>st</sup> tank of DTL was the weak point and most beam loss happened in it. We simulated the beam transporting through the MEBT and the DTL. The initial distribution at the exit of RFQ is obtained with PARMTEQM. The beam current is 15mA and the duty factor is 1.05%. Considering the machine imperfections, alignment, focusing and RF errors are added in simulations as follows for the quadrupole magnets:

- Transverse displacements:  $\delta_{x,y} = \pm 0.1\text{mm}$
- Rotations:  $\phi_{x,y,z} = \pm 3\text{mrad}$
- Integrated field:  $\Delta GL/GL = \pm 1\%$

And for the accelerating field:

- Klystron field:  $\Delta E_{\text{klystron}}/E_{\text{klystron}} = \pm 1\%$
- Klystron phase  $\phi_{\text{klystron}} = \pm 1\text{deg}$
- Gap field:  $\Delta E_{\text{gap}}/E_{\text{gap}} = \pm 1\%$

In 11 out of the 100 runs, particles are lost along the linac and most beam loss concentrated in the 1<sup>st</sup> tank of DTL, where the estimated power lost is higher than the acceptable limit of 1W/m. The excessive beam loss in the 1<sup>st</sup> tank of DTL is due to small bore radius of the tank, which is only 6mm. There are two reasons for us to underestimate beam size and so choose small bore radius: (1) at the beginning of DTL design, beam parameters at the exit of RFQ are adopted and the emittance growth in the MEBT is ignored, which is more than 20%, (2) the K-V distribution is adopted as the initial beam distribution rather than more realistic distribution from PARMTEQM. Based on these analyses, we refined the MEBT and DTL designs. In this study we refer to the initial design as the “old” design and the optimized design as the “new” design.

## MEBT OPTIMIZATION

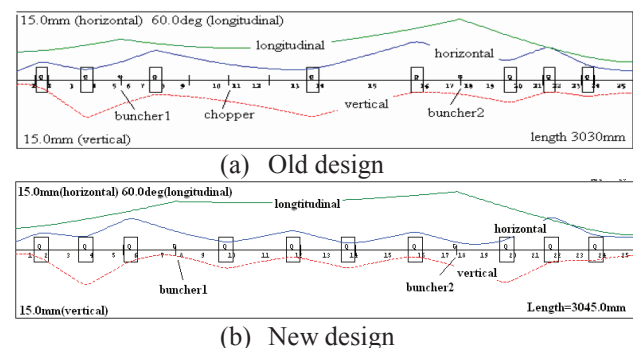


Figure 2:  $6\sigma$  Beam Envelope in MEBT.

Figure 2 shows the 6 times the rms beam envelope for both two MEFT designs obtained by code TRACE-3D [6].

In the old design the MEFT is consisted of 8 quadrupoles, 2 bunchers and 1 chopper, which is to further sharpen the beam edges kept by the pre-chopper. It has been confirmed by the experiment that the beam rise/fall time of the pre-chopper is among 15-20ns[7], which is fully compatible with the physical requirements. Therefore we removed the chopper from MEFT in the new design and add two quadrupole magnets at the position of the chopper. Now the quadrupole magnets in the MEFT are arranged as: two quadrupole magnets are placed at the middle of the MEFT to form a FD focusing period, four quadrupole magnets are placed at the upstream of the MEFT to match the beam output from the RFQ to the FD lattice, four other quadrupole magnets are placed at the downstream of the MEFT to match the beam from the FD lattice into the DTL. There are still two buncher cavities in the new design for longitudinal matching.

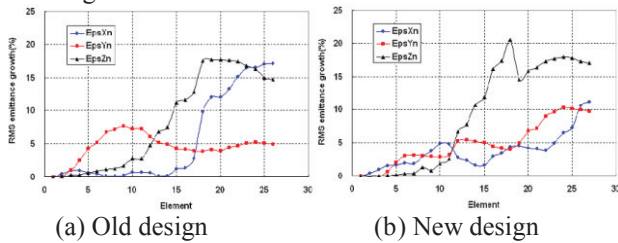


Figure 3: The rms emittance growth in x (dot), y (square) and z (triangle) direction versus the element obtained by code PARMILA.

The rms emittance growth along the MEFT for both two designs is shown in the Figure 3. It is shown that the transverse focusing is more smoothly in the new design and the transverse emittance growth is less than that in the old design.

### DTL OPTIMIZATION

Here, we will illustrate the improvements of the DTL design about geometric parameters and accelerating parameters, and then compare two focusing lattices for the DTL.

#### Geometric Parameters

The old and new designs use the same cell geometries, excluding the beam bore radius and the diameter of drift tubes. To increase the transverse acceptance at the entry of the DTL, the bore radius of the 1<sup>st</sup> tank is enlarged from 6mm to 8mm. To improve the effective shunt impedance, the diameter of drift tubes in the 1<sup>st</sup> and 2<sup>nd</sup> tank is decreased from 148mm to 140mm.

#### Accelerating Parameters

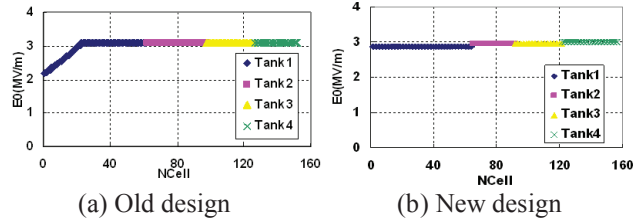


Figure 4: Accelerating electric field along the DTL.

In the old design, the accelerating electric field in the 1<sup>st</sup> tank is ramped from 2.2MV/m to 3.1MV/m over the first 24 cells and then keeps constant. However, this accelerating field law make the tuning difficult, so in the new design, we adopt flat field for all 4 tanks, as shown in Figure 4.

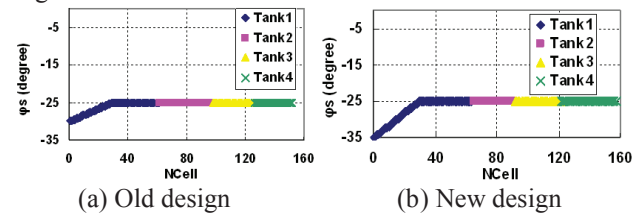


Figure 5: Synchronous phase along the DTL.

In the old design, the synchronous phase is ramped from -30° to -25° over the first 30cells. To increase the longitudinal acceptance in the new design, the synchronous phase is ramped from -35° to -25° over the first 30 cell, as shown in Figure 5.

#### Transverse Focusing

We have study two lattice options to provide focusing: FD and FFDD. The quadrupole gradients for both two lattices were selected to comply with the following design guidelines [8].

1.  $\sigma_{0r} \leq 90^\circ / \text{period}$
2.  $\sigma_{0r} \neq n\sigma_{0l} / 2$ , for  $n=1, 3, \dots$
3. equipartitioning ratio  $\approx 1.0$  at full current

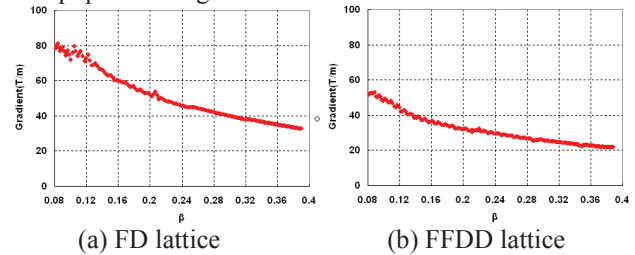


Figure 6: Quadrupole law options.

Figure 6 shows the quadrupole gradients required to meet these constraints for the FD and FFDD lattices. In FD lattice, high quadrupole gradient is required and bigger space is required to accommodate it in drift tubes, which always result to small bore radius and big drift tube diameter.

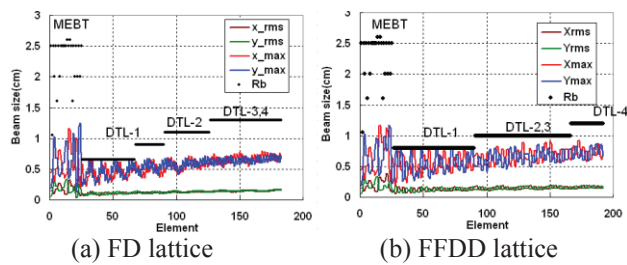


Figure 7: Beam envelope along the linac.

Figure 7 shows the beam envelope along the linac for the FD and FFDD lattices. Compared to the FFDD lattice, the FD lattice can provide stronger focusing, and so the beam envelope oscillating is smoother.

We have studied error effects on beam for the FD and FFDD lattices. With 89% probability the beam loss in the 1<sup>st</sup> DTL tank was less than 1W/m in the FD lattice. However, the probability for beam loss under limit in the 1<sup>st</sup> DTL tank has increased to 96% in the FFDD lattice.

By comparing the transverse performance of both two different transverse focusing lattices, we recommend adopting an FFDD lattice throughout as 1) having the lower expected beam loss in the presence of alignment errors and 2) requiring smaller drift tube space.

## END TO END SIMULATION

After each section of linac has been refined, end-to-end simulation was launched again with PARMILA code. We simulated beam transporting through MEBT, DTL and LRBT. The simulation starts with 15mA H<sup>+</sup> beam output from RFQ obtained with PARMTEQM and ends at the stripping foil in the RCS. 50448 macro-particles per bunch are used. Space-charge interaction is calculated via the 2-dimensional PIC method with a 40×80 mesh. The mesh size is 0.05cm. The bore radius/rms beam size along the MEBT-DTL-LRBT is shown in Figure 8. Its value remains higher than 5.0.

As shown in Figure 9, about 10% of the transverse emittance growth occurs at the MEBT mainly caused by the nonlinear space charge. At the exit of DTL, the transverse emittance growth is about 20% and the longitudinal emittance growth is about 30%. In LRBT, a sudden change of the emittance growth in x-x' plane is visible. It is due to the effect of the dispersion and is compensated by the following bending.

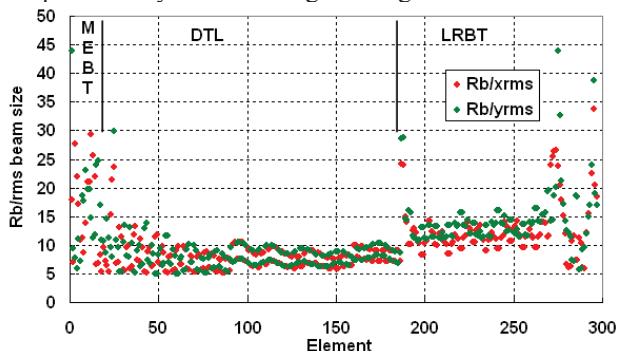


Figure 8: Bore radius/rms beam size along the linac.

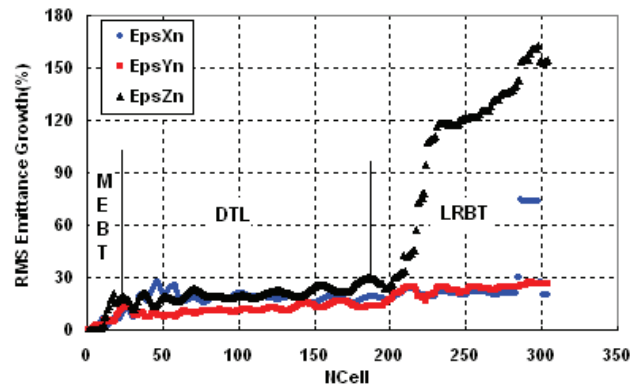


Figure 9: Emittance growth along the linac.

## CONCLUSIONS

Based on some analyses of beam dynamics in CSNS linac, we have refined the MEBT and DTL design. By enlarging the bore radius in the 1<sup>st</sup> DTL tank, the beam loss has reduced. After comparing two different transverse focusing lattices, we finally adopted FFDD lattice for its lower quadrupole gradient and smaller beam loss rate than FD one. End to end simulation has shown that the beam loss, emittance growth rate and the ratio of bore radius to rms beam size were acceptable along the linac and now we reached a final design.

## REFERENCES

- [1] H.F.Ouyang et al, "The High Intensity Proton Linac for CSNS," LINAC2010, Tsukuba, Japan, p.362.
- [2] J. Y. Tang et al. "Beam Transport Lines for the CSNS", EPAC06, Edinburgh, June 2006.
- [3] J.Peng et al, "Design of 132MeV DTL for CSNS," Knoxville, Tennessee USA, p.412.
- [4] T. Harunori. PARMILA, LA-UR-98-4478, 1998, Revised July 26, 2005.
- [5] K.Crandall et al, RFQ Design Codes, LA-UR-96-1836 (1998).
- [6] K.Crandall et al, LA-UR-97-886.
- [7] H.Liu et al. Nuclear Instruments and Methods in Physics Research A 654(2011) 2-7.
- [8] J. Stovall et al, "Quadrupole Law and Steering Options in the Linac4 DTL," sLHC Project Note 0006.